NASA Technical Memorandum 107106

# Determination of Local Densities in Accreted Ice Samples Using X-Rays and Digital Imaging

Howard Broughton and James Sims
*Cortez III Service Corporation*
*Cleveland, Ohio*

Mario Vargas
*Lewis Research Center*
*Cleveland, Ohio*

Prepared for the
48th Annual Conference
sponsored by the Society for Imaging Science and Technology
Washington, DC, May 7–12, 1995


National Aeronautics and
Space Administration

# Determination of Local Densities in Accreted Ice Samples using X-rays and Digital Imaging

*Howard Broughton, James J. Sims*
*Cortez III Service Corporation, Brook Park, Ohio*

*Mario Vargas*
*NASA Lewis Research Center, Cleveland, Ohio*

## ABSTRACT

At the NASA Lewis Research Center's Icing Research Tunnel ice shapes, similar to those which develop in-flight icing conditions, were formed on an airfoil. Under cold room conditions these experimental samples were carefully removed from the airfoil, sliced into thin sections, and x-rayed. The resulting microradiographs were developed and the film digitized using a high resolution scanner to extract fine detail in the radiographs. A procedure was devised to calibrate the scanner and to maintain repeatability during the experiment. The techniques of image acquisition and analysis provide accurate local density measurements and reveal the internal characteristics of the accreted ice with greater detail. This paper will discuss the methodology by which these samples were prepared with emphasis on the digital imaging techniques.

## INTRODUCTION

Part of the Icing Research Program at NASA Lewis Research Center involves the study and measurement of local and total densities of ice shapes accreted on airfoils. Density measurements are needed to study the structure and formation of ice and to evaluate density correlations employed in computer applications that model ice accretion.

This report presents the imaging methodology employed to obtain local densities in ice shapes accreted on airfoils at the NASA Lewis Icing Research Tunnel (IRT). The methodology takes advantage of modern imaging techniques to improve and extend F. Prodi's [1,2] x-ray contact microradiography method of measuring ice density. In the past, measurements of accreted ice density have mainly been performed using the rotating multi-cylinder technique, [3,4] but there are difficulties in extending the results to non-rotating bodies such as airfoils [5]. A methodology is needed to measure local and total densities of accreted ice shapes on airfoils. Prodi's technique, although originally applied to hailstones, can be improved and extended to measure local and total densities in ice shapes accreted on airfoils by using recent technical advances in imaging.

The methodology described in this paper was applied to ice shapes that were accreted on a NACA 0012 airfoil in the IRT for a range of icing conditions. The shapes were then removed from the airfoil and cut into thin slices. X-rays were then used to obtain a contact microradiograph of each slice. The developed film was digitized and image processing techniques were used to measure the density of the film which was correlated to the physical density of the ice (see Figure 1).

Applications of the methodology are presented for a rime ice, glaze ice, and a mixed ice case. For the mixed and rime ice cases local densities are measured across a region of the ice shape and image processing techniques are used to obtain information on the structure of the ice.

## EXPERIMENTAL

Ice shapes were accreted on an NACA 0012 airfoil in the Icing Research Tunnel [6] (see Figure 2) at the NASA Lewis Research Center for a range of icing conditions. The ice shapes were removed from the airfoil, wrapped in plastic and stored in a freezer. When enough ice samples were collected, the temperature in the tunnel was lowered to 0° F, the air flow stopped and the tunnel used as a cold room. The experimental hardware was moved inside the tunnel and allowed to chill until it reached tunnel ambient temperature. The ice samples were then removed from the freezer and cut to approximately 10 mm thickness with a band saw.

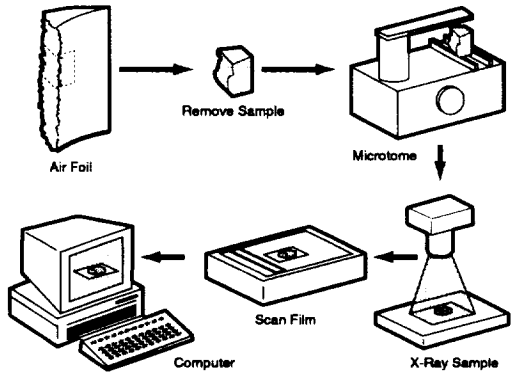


*Figure 1: Experimental schematic*

To mount the thick slices onto the microtome a method was developed in which an aluminum plate was placed on a heating pad and an icy fingerprint was imprinted on it. When the plate reached the temperature where the fingerprint was beginning to melt the plate was removed and the sample placed on it. The plate was immediately placed on a large steel block which acted as a cold sink. The thin liquid film froze immediately creating a very strong bond. Extreme care was exercised to keep the thin film to a minimum to avoid contamination of the sample.

One side of the sample was microtomed creating a flat surface, then the sample was flipped over and the reverse side microtomed. Since the mounting plate was parallel to the cutting blade both surfaces of the ice sample were also parallel. As the sample neared the 3 mm depth it was measured at eight locations around the perimeter with a depth gage until the desired thickness was obtained.

Once the sample was determined to be 3 mm it was removed from the mounting block. The instant the sample became free from the block it was carefully placed on a sheet of mylar used to transfer it to the x-ray source. The x-ray device was fabricated from a photographic enlarger with an attached easel base (see Figure 3). A Watkin-Johnson x-ray source was used with a maximum output power of 50 kV and a maximum output current of 1 mA was used. For safety reasons the x-ray device was shielded on three sides with 1/4 inch aluminum plates to block scattered rays.

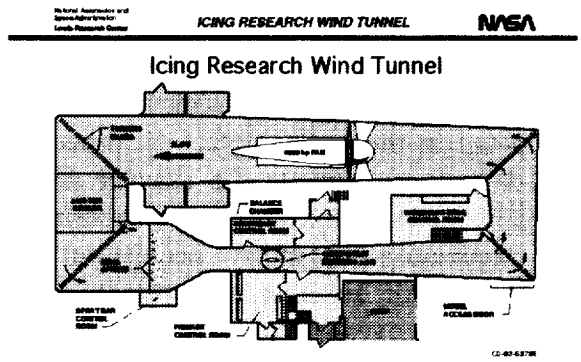


*Figure 2: Schematic of Icing Research Tunnel*

Kodak Industrex ready pack II type M x-ray film was used because of its high resolution and sealed packaging. The film was held in place by the easel and the sample placed in contact with the film packet. Prior to exposure the x-ray device was run for several minutes to warm up and reach a stable operational mode. Exposure was determined in the pretest phase of the experiment ensuring the density of the film was within the dynamic range of the film scanner. An input current of 1 mA and 25 kV exposing the film for 30 seconds produced sufficient density.

A reference sample of clear ice made from distilled, de-ionized water was placed in the

corner of each radiograph exposed. This reference sample was also microtomed to 3 mm with co-planar sides and served to calibrate the digital images.

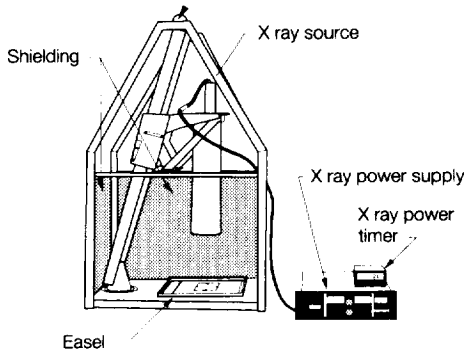


*Figure 3: X-ray device*

Non-uniformities in the x-ray source caused density variations in the film which would affect the localized density measurements. To compensate a series of flat field images (see Figure 4) were exposed each day of the experiment. The flat field image is exposed under the x-ray source without a sample and digitally subtracted from the sample image (see Figure 5). During the experiment, flat fields were exposed in between each sample image to monitor shifts in the non-uniformity and to provide an average flat field over time. Processing of the film was performed with a Kodak X-Omat radiographic film processor at the recommended time and temperature.

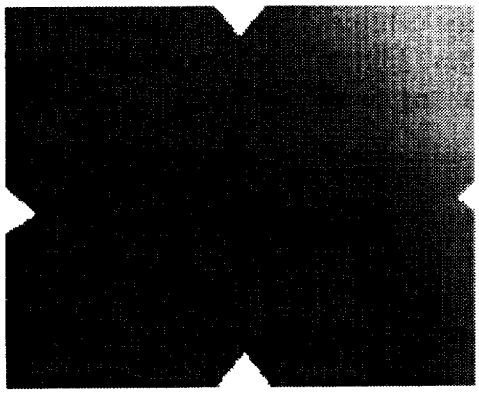

*Figure 4: Flat field image*

The radiographs were scanned with a Leafscan-45 film scanner at a resolution of 1100 pixels per inch (ppi) creating a 19 MB file. Four v-shaped registration marks were exposed on each sheet of film facilitating registration of each image. A registration mark on each side of the film served as a backup if one shifted. By having several registration marks any two or all could be used to insure registration accuracy.

Prior to the experiment the film scanner was tested to evaluate its consistency from scan to scan. It was found that the scanner auto-ranged the output gray values based on the radiograph density range. The auto-ranging changed the internal lookup table based on the minimum and maximum intensity value of the pre-scanned image, thereby expanding the dynamic range of the output image. To circumvent the auto-ranging feature a balanced target was pre-scanned, in this case a Kodak gray scale, which provided the same minimum and maximum intensity value for each subsequent scan.

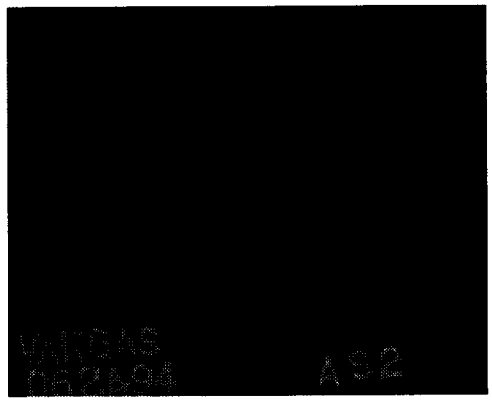

*Figure 5: Sample Image with subtracted flat field*

Registration was performed using two of the four registration marks (see Figure 6) and checked against the other two. Each registration mark was enlarged sufficiently to locate the end point. This was determined accurately by counting the cross-sectional profile of pixels across the registration point and selecting the midpoint pixel. Then counting the pixels from the edge of the film to the same midpoint pixel and using these values as a standard measurement for the entire experiment. Shifting the images so each midpoint pixel resided at the same spatial location effectively registered each image to another. The displacement of opposite registration marks were

checked to verify proper alignment when scanned. If this varied by more than five pixels the radiograph was realigned in the film holder and rescanned. Other point to point calculations were used to monitor shrinkage and swelling of the film which was found to be negligible.

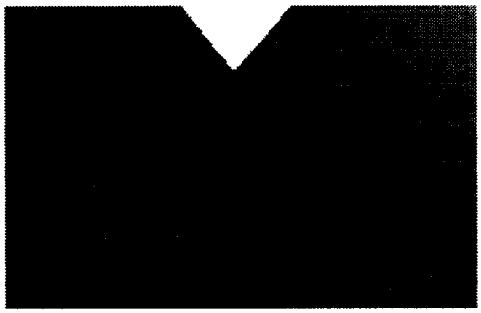

*Figure 6: Magnified registration mark*

Once all of the radiographs were scanned and registered, the flat field images for that particular day were averaged together into a single flat field image $g(x,y)$. Where $fd_i(x,y)$ is each flat field image.

$$g(x,y) = \frac{1}{N}\sum_{i=1}^{N} fd_i(x,y) \qquad (1)$$

The averaged flat field image was then subtracted from all of the sample images $s(x,y)$ which resulted in the sample image $s'(x,y)$ with corrected intensity values.

$$s'(x,y) = s(x,y) - g(x,y) \qquad (2)$$

To correlate the system from physical ice density to digital intensity values there must exist a known density region in the x-rayed image. Each sample was exposed with the reference ice sample for calibration. Since the reference sample was produced with extremely clean water it was assigned the value of 0.917 gm cm$^{-3}$. This assumption served as the correlation point for all of the digital images in the experiment.

The density value assigned to the reference sample made it possible to associate the digital intensity values to the physical density of the ice sample. Several hundred pixels from the reference sample region were averaged resulting in a single intensity value. The conversion process was accomplished by making a global adjustment to the digital image, setting the average intensity value $b$ of the reference sample equal to 0.917 gm cm$^{-3}$ resulting in the corrected density image $\rho(x,y)$.

$$\rho(x,y) = 0.917\left[\frac{s'(x,y)}{b}\right] \qquad (3)$$

where $b$ is the average intensity value of the reference sample represented by

$$b = \frac{1}{N}\sum_{i=1}^{N} r_i(x,y) \qquad (4)$$

This procedure converted all of the raw intensity values of the digital image into values that represent the actual ice sample densities.

## RESULTS

The microradiographs reveal density variations within the sample that would have normally been concealed from the naked eye. Digitizing the samples allowed image processing techniques to evaluate ice formation and morphological anomalies. Since the density of each pixel, as it relates to the reference sample, was known the image could be thresholded at specific densities revealing unobserved characteristics. Figure 7 shows a sample of glaze ice containing air bubbles.

*Figure 7: Image of glaze ice sample*

*Figure 8: Thresholded sample to show air pockets (glaze ice)*

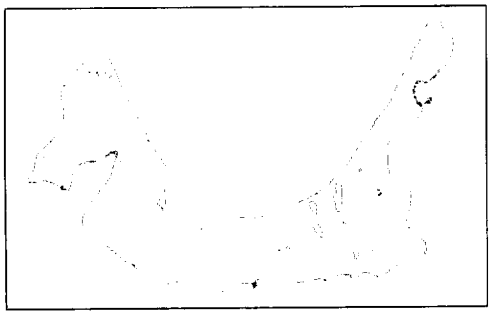

*Figure 9: Glaze ice image with edge detection*

Figure 8 shows the same image thresholded to show the morphology of the sample. The advantage of this technique allows one to analyze the images with a resolution up to 256 distinct densities and a spatial resolution of 1100 density measurements per inch. Figure 9 shows how edge detection can be utilized to evaluate air pocket characteristics.

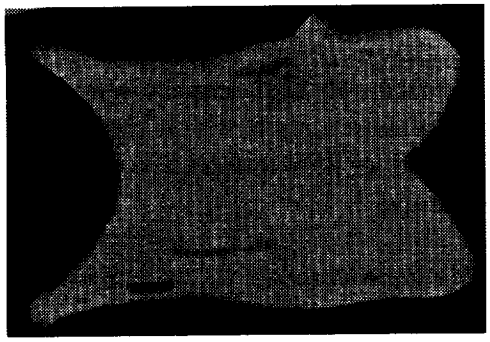

*Figure 10: Image of mixed ice sample*

Figure 10 is a typical example of a mixed ice sample. The thresholded mixed ice sample in Figure 11 shows air pockets along the periphery.

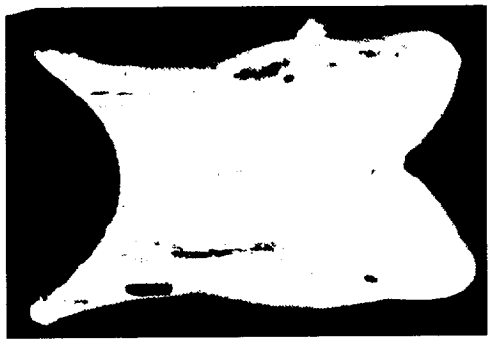

*Figure 11: Thresholded sample to show air pockets (mixed ice)*

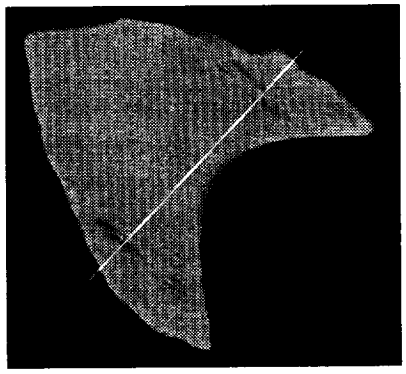

*Figure 12: Image of rime ice sample with profile line*

The rime ice sample in Figure 12 shows distinct morphological characteristics. The intensity profile in Figure 13 shows that these are portions with lower density values and indicate air bubbles in the ice structure. Figure 14 shows the thresholded rime ice sample.

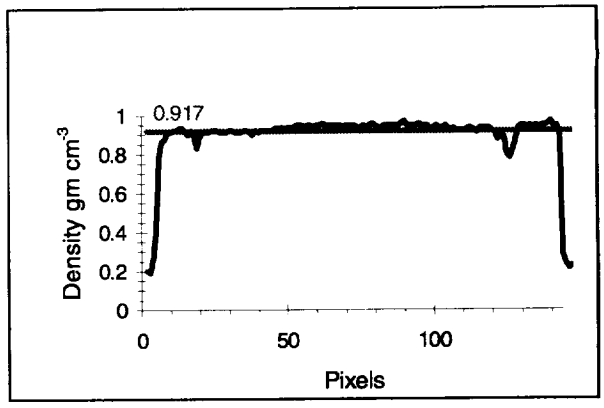


*Figure 13: Profile of density values for rime ice*

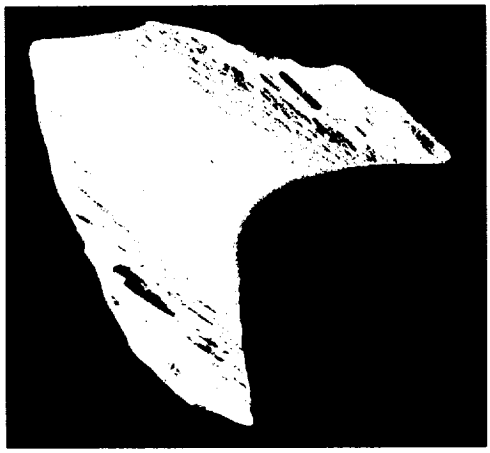

*Figure 14: Thresholded rime ice sample*

This experiment demonstrates that x-rays and digital image processing can improve the analysis of density variations in accreted ice samples. Using the method described it was possible to analyze the density variations throughout the sample and identify characteristics imperceptible prior to this experiment. The improvement in resolution over Prodi's method significantly enhances the data gathering capabilities. Prodi used a microdensitometer with an aperture size of 0.4 mm and a sampling interval of 0.5 mm. In this experiment each pixel represented a 23 micron aperture size with an evenly spaced 23 micron sampling interval. Our spatial resolution was 17 times finer than the microdensitometer used by Prodi.

In addition to improving resolution, digital imaging provides repeatability in measurements and absolute positional accuracy. With this ability verifying a measurement or analysis is simple and effective. Another significant aspect of digital imaging is eliminating the necessity of handling the original radiographs for each measurement. The radiograph is scanned once and stored, leaving the digital image for analysis. All of the digital images were recorded onto CD-ROM. This has the advantage of providing a convenient means to retrieve, analyze, and archive the data. CD-ROM is advantageous for archiving because it bypasses the impermanence issues associated with silver halide systems.

**DISCUSSION**

A digital method was applied to evaluate accreted ice densities by making local and average densities measurements. This technique shows that the resolution of the imaging system is adequate to evaluate the structure and density characteristics of icing growth. It is felt that the use of digital imaging provides the ability to make repeatable and precise measurements.

Variability can be attributed to basically two areas; the variation in thickness of the samples and the quantization of density values. The thickness of the sample was measured in eight locations around the perimeter during the microtoming process. However, it was noticed that blade of the microtome flexed a minuscule amount from the mounted portion to the end of the blade when attempting to shave more than 15 microns in a single pass. This resulted in the sample having a sloped surface. By decreasing the amount of distance the blade dropped, thus shaving less of the sample on each pass, the blade flex was reduced almost to the point of elimination providing parallel surfaces.

Quantization error could effectively be reduced by utilizing more than 8 bits of information, thus providing a wider dynamic range. The Leafscan-45 film scanner outputs 8 and 16 bits of information which results in a dynamic range of 256, and 65,536 density values respectively.

Possible improvements to the experiment may be realized by utilizing an additional reference sample impervious to variability. This reference sample, made from thin metal or plastic, would be used to monitor potential thickness variation in the ice reference sample.

## References

1. Prodi, F.: Measurement of Local Density in Artificial and Natural Hailstones. *J. Appl. Meteor.*, Vol.9, Dec.1970, p. 903-910

2. Prodi, F: X-Ray Images of Hailstones *J. Appl. Meteor.* ,Vol.8, June.1969, p. 458-459

3. Jones, K.F.: The Density of Natural Ice Accretions Related to Non-Dimensional Icing Parameters. *Q.J.R.Meteorol.Soc.* Vol. 116, 1990, p. 477-496

4. Macklin, W.C.: The Density and Structure of Ice Formed by Accretion, *Q.J.R.Meteorol.Soc.* Vol. 88, 1962, p. 30-50

5. Rios, M.A.: Icing Simulations Using Jones' Density Formula for Accreted Ice and LEWICE, AAIA-91-0556

6. Soeder, R.H. and Andracchio, C. R.: NASA Lewis Icing Research Tunnel User Manual, NASA TM-102319, June 1990

### Acknowledgments

The authors would like to thank Gary Nolan and Janet Ivancic for their assistance in the digital imaging portions of the experiment. Special thanks to Clark Hahn for sharing his expertise in x-ray imaging and for donating equipment for the experiment.

## APPENDIX

Correlation of the density (blackness) of the film with the actual physical density of the ice sample is done following Prodi's methodology[2].

If we have a parallel monochromatic X-ray beam of intensity $I_o$ incident on the ice sample and on the film plate (Figure A1), we call $X_A$ the thickness of a region of the ice free of voids (air bubbles), $\rho_I$ the density of the ice in this region, $I_A$ the transmitted intensity, and $D_A$ the density of the film due to the exposure to the transmitted intensity.

In a region of the ice containing air bubbles, $X_A$ is still the thickness of the ice sample (sample assumed to have parallel faces), $X_B$ is the true thickness of the material (thickness of the material less voids), $\rho_H$ is the density of the ice in this region, $I_B$ is the transmitted intensity, and $D_B$ is the density of the film due to the exposure to the transmitted intensity.

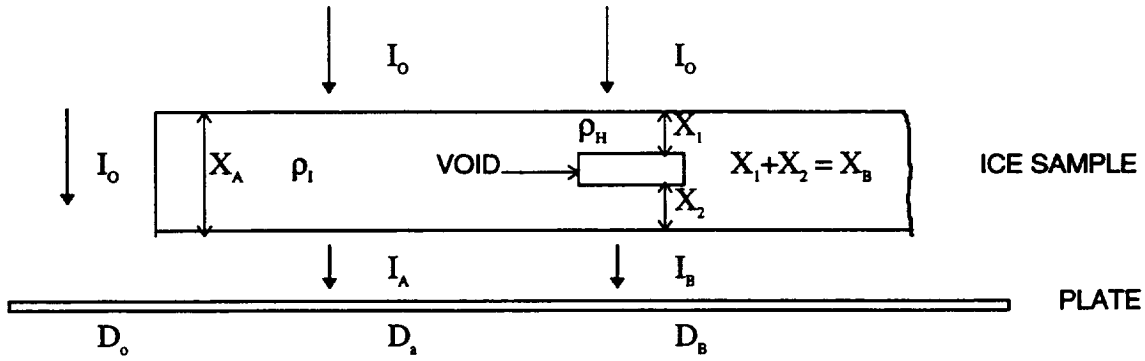


FIGURE A1

The ratio of the density can be related to the ratio of the thickness of the two regions:

$$\rho_H = m_B / X_A \qquad \text{(A1)}$$

where $m_B$ is the mass contained in volume $X_A \cdot 1 \cdot 1$ in the region with air bubbles. But $m_B$ can be expressed as:

$$m_B = \rho_I X_B$$

then

$$\rho_H = \rho_I X_B / X_A$$

and

$$\rho_H / \rho_I = X_B / X_A \qquad \text{(A2)}$$

The ratio of the thickness $X_A / X_B$ can be related to the beam intensity using Lambert's law:

$$I = I_o \exp(-\sigma X) \qquad \text{(A3)}$$

where $I_o$ and I are the incident and transmitted radiation respectively, $\sigma$ is the absorption coefficient of the material, and X is the thickness.

From (A3) $$X = -1/\sigma \ln(I/I_o) \quad (A4)$$

and $$X_B/X_A = \ln(I_o/I_B)/\ln(I_o/I_A) \quad (A5)$$

where the coefficient of absorption has been canceled out, assuming the ice is homogeneous wherever there are no bubbles.

Substitution of (A5) into (A2) gives:

$$\rho_H/\rho_I = \ln(I_o/I_B)/\ln(I_o/I_A) \quad (A6)$$

Photographic exposure E can be expressed as:

$$E = It \quad (A7)$$

where t is the exposure time. The response characteristic of the film for a certain photographic emulsion is defined as:

$$\gamma = D/\log E = D/\log(It) = D/(\log I + \log t) \quad (A8)$$

where $$\log I = (D - \gamma \log t)/\gamma \quad (A9)$$

If we operate in the linear region of the film where $\gamma$ is constant, then

$$\rho_H/\rho_I = [((D_o - \gamma \log t)/\gamma) - ((D_B - \gamma \log t)/\gamma)] / [((D_o - \gamma \log t)/\gamma) - ((D_A - \log t)/\gamma)]$$

$$\rho_H/\rho_I = (D_o - D_B)/(D_o - D_A)$$

where $D_o$ ,$D_A$ , $D_B$ , are respectively the measured photographic density in the region clear of the sample, in the region where the ice is clear of bubbles, and in the region where the ice contains bubbles.

The local density of the ice sample in a given location can be obtained if we know the density at a location within the sample where the ice is clear of bubbles, and if we measure the film density at three locations: in a region where the ice is clear of bubbles, in a region of the film away from the sample, and in the region where we want to measure the physical density of the ice:

$$\rho_H = \rho_I (D_o - D_B)/(D_o - D_A)$$

# REPORT DOCUMENTATION PAGE

*Form Approved*
*OMB No. 0704-0188*



| 1. AGENCY USE ONLY (*Leave blank*) | 2. REPORT DATE | 3. REPORT TYPE AND DATES COVERED |
|---|---|---|
| | March 1996 | Technical Memorandum |

**4. TITLE AND SUBTITLE**

Determination of Local Densities in Accreted Ice Samples Using X-Rays and Digital Imaging

**5. FUNDING NUMBERS**

WU-505-68-10

**6. AUTHOR(S)**

Howard Broughton, James J. Sims, and Mario Vargas

**7. PERFORMING ORGANIZATION NAME(S) AND ADDRESS(ES)**

National Aeronautics and Space Administration
Lewis Research Center
Cleveland, Ohio 44135-3191

**8. PERFORMING ORGANIZATION REPORT NUMBER**

E-10002

**9. SPONSORING/MONITORING AGENCY NAME(S) AND ADDRESS(ES)**

National Aeronautics and Space Administration
Washington, D.C. 20546-0001

**10. SPONSORING/MONITORING AGENCY REPORT NUMBER**

NASA TM-107106

**11. SUPPLEMENTARY NOTES**

Prepared for the 48th Annual Conference sponsored by the Society for Imaging Science and Technology, Washington, DC, May 7-12, 1995. Howard Broughton and James J. Sims, Cortez III Service Corporation, 21000 Brookpark Road, Cleveland, Ohio 44135 (work funded by NASA Contract NAS3-24816); Mario Vargas, NASA Lewis Research Center. Responsible person, Mario Vargas, organization code 2720, (216) 433-3943.

**12a. DISTRIBUTION/AVAILABILITY STATEMENT**

Unclassified - Unlimited
Subject Category 01

This publication is available from the NASA Center for Aerospace Information, (301) 621-0390.

**12b. DISTRIBUTION CODE**

**13. ABSTRACT** (*Maximum 200 words*)

At the NASA Lewis Research Center's Icing Research Tunnel ice shapes, similar to those which develop in-flight icing conditions, were formed on an airfoil. Under cold room conditions these experimental samples were carefully removed from the airfoil, sliced into thin sections, and x-rayed. The resulting microradiographs were developed and the film digitized using a high resolution scanner to extract fine detail in the radiographs. A procedure was devised to calibrate the scanner and to maintain repeatability during the experiment. The techniques of image acquisition and analysis provide accurate local density measurements and reveal the internal characteristics of the accreted ice with greater detail. This paper will discuss the methodology by which these samples were prepared with emphasis on the digital imaging techniques.

**14. SUBJECT TERMS**

Ice; X-ray; Digital imaging

**15. NUMBER OF PAGES**

11

**16. PRICE CODE**

A03

| 17. SECURITY CLASSIFICATION OF REPORT | 18. SECURITY CLASSIFICATION OF THIS PAGE | 19. SECURITY CLASSIFICATION OF ABSTRACT | 20. LIMITATION OF ABSTRACT |
|---|---|---|---|
| Unclassified | Unclassified | Unclassified | |

National Aeronautics and
Space Administration

**Lewis Research Center**
21000 Brookpark Rd.
Cleveland, OH 44135-3191